C. R. Chimie 18 (2015) 1123–1133

Contents lists available at ScienceDirect

Comptes Rendus Chimie

www.sciencedirect.com

International Symposium on Air & Water Pollution Abatement Catalysis (AWPAC) – Catalytic pollution control for stationary and mobile sources

Synthesis of Faujasite type zeolite from low grade Tunisian clay for the removal of heavy metals from aqueous waste by batch process: Kinetic and equilibrium study

Synthèse d'une zéolithe de type faujasite à partir d'une argile commune tunisienne pour l'élimination des métaux lourds contenus dans des déchets aqueux par un traitement par batch : étude cinétique et de l'équilibre

Olfa Ouled Ltaief [a], Stéphane Siffert [b,*], Sophie Fourmentin [b], Mourad Benzina [a,*]

[a] *Water, Energy and Environment Laboratory, Code AD 10-02 ENIS, BP 3038 Sfax, Tunisia*
[b] *ULCO, Unity of Environmental Chemistry and Interactions on the Living Organisms (UCEIV), EA4492, 59140 Dunkerque, France*

ARTICLE INFO

Article history:
Received 28 November 2014
Accepted after revision 30 March 2015
Available online 7 September 2015

Keywords:
Adsorbent
Tunisian clay
Zeolite
Adsorption isotherms
Heavy metals

Mots clés :
Adsorbant
Argile tunisienne
Zéolithe
Isothermes d'adsorption
Métaux lourds

ABSTRACT

In this study, a faujasite type zeolite synthesized from cheap local Tunisian illitic clay and having a hierarchical porosity was used for adsorption of heavy metals. The adsorption behavior of the FAU with respect to Cu (II), Cr (III) and Co (II) has been investigated using batch experiments. The removal efficiency was determined at different contact times, initial metal concentrations, temperatures, pHs, and adsorbent amounts. Both Langmuir and Freundlich isotherms fit well with the equilibrium data. Kinetic studies showed that the adsorption followed a pseudo-second-order model. The observed selectivity was determined as follow: Cu (II) > Co (II) > Cr (III).

RÉSUMÉ

Une zéolite de type faujasite ayant une porosité hiérarchisée a été synthétisée à partir d'une argile tunisienne. Les capacités d'adsorption de cette zéolite ont été évaluées vis-à-vis de la rétention de métaux lourds : Cu (II), Cr (III) et Co (II). L'influence de divers paramètres tels que le temps, la concentration, la température, le pH et la quantité d'adsorbant a été étudiée. Les résultats obtenus ont montré que les modèles de Langmuir et Freundlich décrivaient bien l'adsorption des métaux étudiés et que l'adsorption suivait un modèle cinétique du deuxième ordre. La sélectivité observée suit l'ordre : Cu (II) > Co (II) > Cr (III).

* Corresponding authors.
E-mail addresses: siffert@univ-littoral.fr (S. Siffert), Mourad.Benzina@enis.rnu.tn (M. Benzina).

http://dx.doi.org/10.1016/j.crci.2015.03.013
1631-0748/

1. Introduction

The contribution of heavy metals to ecosystems has a negative impact on human health and the environment [1]. Heavy metals are not biodegradable and tend to accumulate in living organisms causing several troubles [2]. Heavy metals such as copper (Cu) (II), chromium (Cr) (III) and cobalt (Co) (II) are prior toxic pollutants in water. Indeed, the presence of excess of those metals in drinking water could cause many diseases [3].

In fact, Cu ions can deposit in brain, skin, liver, pancreas and myocardium causing severe toxicological effects on humans and animals [3]. High concentrations of cobalt can also cause several health troubles, like low blood pressure, lung irritations, paralysis, and diarrhea and may cause genetic changes in living cells [4]. Likewise, when Cr (III) concentration in drinking water is above a critical degree, it becomes toxic and can cause structural perturbation in the human erythrocyte membrane in a more important way than Cr (VI). It can change the biological membrane permeability, which affects the function of ion channels and enzymes found in the erythrocyte membranes [5]. Therefore, those heavy metals have to be eliminated from wastewaters before they are given to the receiving medium.

In the last decades, several methods, such as precipitation, reverse osmosis, coprecipitation, ion-exchange, membrane electrolysis, oxidation, and adsorption were exploited to remove heavy metals from aqueous solutions [6–9]. Among these methods, adsorption is regarded as the most efficient choice when both environmental and economic factors are considered [10]. Among available adsorbent, zeolites were evaluated to be better than clays, sands and activated carbons. Moreover, zeolites are playing a significant role in wastewater processing seeing that they are reputed for their stability toward temperature, ion-exchange properties, high porosity and sieving properties [11].

Zeolites are microporous crystalline hydrated aluminosilicates characterized by a three-dimensional network of tetrahedral (Si, Al)O_4 units that form a system of interconnected pore. Thanks to their similar structure and physicochemical properties, synthetic zeolites have replaced natural zeolites in many applications. Synthetic zeolites can be prepared from a number of source materials, and clay material is one of the most often used for this purpose [12–14]. Several methods have been reported to synthesize zeolites including hydrothermal synthesis, microwave synthesis and vapor synthesis. The fusion method suggested by Shigemoto et al. [15] which includes an alkaline fusion stage prior to the conventional hydrothermal process, has been evaluated as an effective method that can turn clay material into high pure zeolite [15]. Zeolites synthesized from clay could then be used for the removal of heavy metals from soil and contaminated aqueous solutions [16–18].

The present study investigated the ability of a synthesized faujasite type zeolite (FAU) from Tunisian clay material to remove heavy metals (Co, Cr and Cu) from aqueous solutions. Indeed, owing to their interesting textural properties (lamellar structure, high surface area and large cation exchange capacity), natural and modified Tunisian clay materials have shown great potential to remove pollutants, from aqueous solution [19] as well as from gaseous effluent [20,21]. The synthesized faujasite type zeolite having a hierarchical porosity should present particular abilities for adsorption. The influences of adsorbent dosage, contact time, pH value, initial metal concentration, and temperature were evaluated to fix the optimal uptake conditions. The equilibrium isotherms and adsorption kinetics of the removal of those three metals by the FAU were also studied.

2. Materials and methods

2.1. Materials

Illitic clay (IC) used in this study was obtained from Jebel Khcham Rbib deposits located in the region of El Hamma-Gabes, Tunisia. $CuSO_4{\cdot}5H_2O$, $CoCl_2{\cdot}6H_2O$, $K_2Cr_2O_7$ and 98% NaOH (analytic reagent grade) were purchased from Fluka Chemical. The results of our synthesized FAU zeolite will be compared with a commercial one purchased from "Zeolyst International CBV100". The zeolite was of Na-faujasite type with: a Si/Al ratio of 2.7, a total pore volume of 0.291 cm^3/g and a specific surface area of 731 m^2/g.

2.2. Optimal synthesis of faujasite type zeolite

Firstly, IC was crushed and grinded to obtain powder with particle size diameter less than 50 μm. IC was then mixed with NaOH powder. The resulting material was grinded, placed in a nickel crucible and heated in a muffle furnace. The fused sample was then cooled to room temperature, grinded to a fine powder, and added to the appropriate amount of distillated water, followed by vigorous stirring at room temperature. The obtained gel was then transferred into stainless autoclave and crystallized at 60 °C for 24 h. Finally, the solid product was separated by filtration and washed thoroughly several times with deionized water until the pH reached around 9, then it was dried and crushed.

2.3. Characterization of the zeolite

The mineralogical characterization of the FAU was carried out by X-ray diffraction [Bruker AXS D8 Advance diffractometer equipped with a copper anode (λ = 1.5406 Å)]. Data collection was carried out in the range 5–60 with a step size of 0.02. Phase identification was performed by searching the ICDD powder diffraction file database, with the help of Joint Committee on Powder Diffraction Standards (JCPDS) files. Morphological observations were performed using a 438 VP microscope (LEO, Cambridge UK) equipped with an energy dispersive X-ray spectrometer (IXRF, USA) (SEM EDX). Nitrogen adsorption–desorption experiments were carried out at 77 K on a Sorptomatic 1990 series apparatus. The sample was degassed at 200 °C prior to measurement. The surface area was determined using Brunauer–Emmett–Teller (BET) method.

2.4. Batch adsorption studies

The adsorption of Co (II), Cu (II) and Cr (III) onto FAU were carried out in laboratory using batch reactor. A volume of 100 mL of each metal solution with a known amount of zeolite was placed in an Erlenmeyer flask to start the experiments. Different initial metal ion concentrations ranging from 10–150 mg/L, pH values (2–9), FAU amount (0.01–0.8 g), temperature (25–45 °C) and retention times (15–240 min) were studied. At the end of each experience, the adsorbent was removed by filtration, while the equilibrated metal concentration was evaluated in the filtrate by atomic absorption spectrophotometry (Varian AA 20). Amounts of metals extracted by the FAU were calculated as:

$$q_e = \frac{(C_0 - C_e)V}{m} \quad (1)$$

where q_e is the amount of the metal ions adsorbed on the FAU (mg/g), C_0 is the initial aqueous metal ions concentration (mg/L), C_e is the equilibrium aqueous concentration of metal ions (mg/L), V is the volume (L), and m the amount of FAU (g).

3. Results and discussion

3.1. Characterization of the synthesized material

Fig. 1 shows X-ray patterns of the obtained zeolite. According to the diffractogram, the prepared material presented only one phase of a pure faujasite type zeolite. The typical reflection peaks of kaolinite and illite disappeared, indicating that the structure of IC was destroyed. This could be attributed to the fusion step that can easily dissolve those components for FAU formation in the later stage of hydrothermal synthesis with transformation of IC into faujasite type zeolite. Morphological analyses of the FAU (Fig. 1) showed zeolitic crystals, which exhibit well-defined hexagonal morphology.

The nitrogen isotherms of the synthesized FAU are depicted on Fig. 2. We can notice the presence of a steep in the nitrogen uptake at very low relative pressures ($P/P_0 = 0.02$) attributed to the filling of micropores. An obvious type H_4 hysteresis loop (from 0.40 to 0.85) is observed, corresponding to the filling of uniform slit-shaped intercrystal mesopores, which arise from the packing of zeolite nanocrystals. Another uptake appears at high relative pressure (0.85–1.0), which is assigned to the filling of macropores formed by the packing of aggregated particles [22]. Thus, the FAU synthesized from IC has a trimodal macro-meso-microporous structure.

The specific surface area and total pore volume were found to be equal to 360 m^2/g and 0.33 cm^3/g, respectively. Textural properties of the FAU are summarized in Table 1.

3.2. Heavy metal removal evaluation

The removal of heavy metal ions on Faujasite has been widely studied. Adsorption was attributed to different mechanisms of ion-exchange processes as well as adsorption process [23–25]. During the ion-exchange process, metal ions move through the pores and channels of zeolite and replace exchangeable cations (mainly sodium). The diffusion is faster through the pores and is retarded when the ions move through the smaller channels.

3.2.1. Effect of FAU amount

The sorption of metal ions on the synthesized FAU was investigated on various amounts of sorbents (from 0.01 to 0.8 g) in constant solution volume (100 mL) at constant

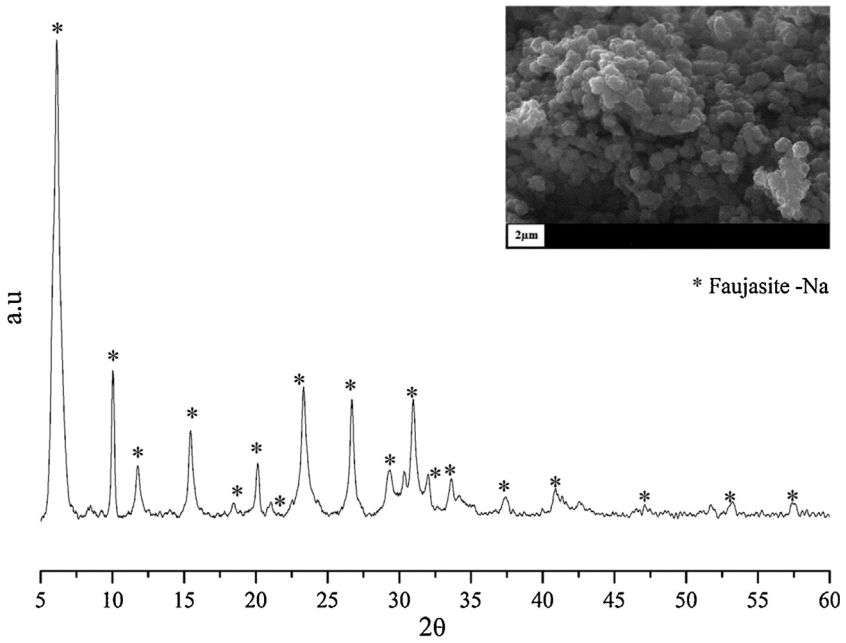

Fig. 1. X-ray diffraction pattern and SEM micrograph of the faujasite type zeolite.

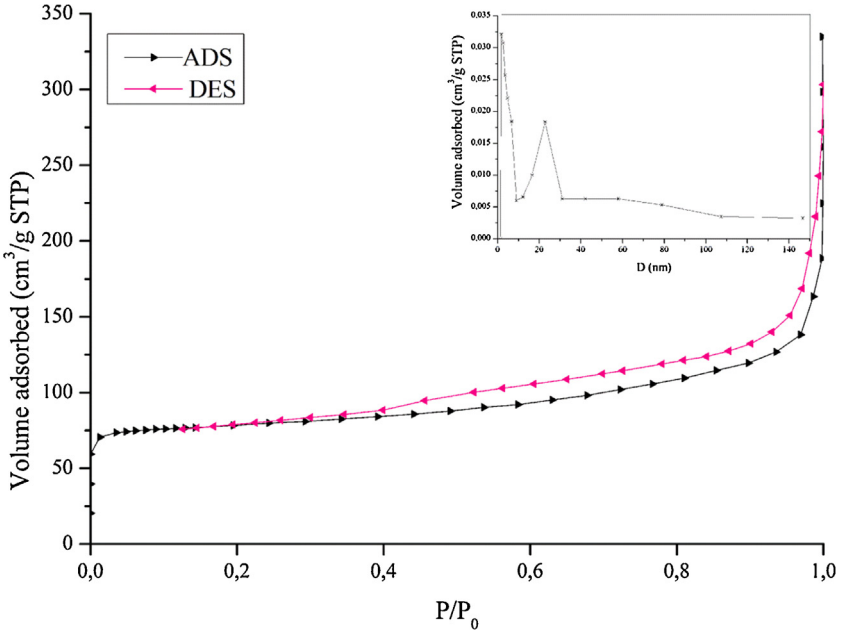

Fig. 2. (Color online.) N_2 adsorption–desorption isotherms and Barett, Joyner and Halenda (BJH) pore size distribution of the faujasite type zeolite.

room temperature (25 °C) and constant metal concentration (50 mg/L). The results obtained are illustrated on Fig. 3, which shows that the removal percentage increased considerably with the increasing amount of the sorbent up to 0.05 g/100 mL for all tested metals. This is due to the larger availability of the exchangeable adsorption sites at the available greater sorbent surface area [23,26]. However, further increases in the dose of sorbent did not lead to an increase in the percentage of removal, which could be attributed to saturation of the binding sites [27]. Based on these results, 0.05 g/100 mL was chosen as the optimum dosage for Cu (II), Co (II) and Cr (III) with a removal efficiency of 93%, 92% and 68%, respectively. In comparison with other studies reported in literature for heavy metal removal, we can concluded that in the present study we have optimized the zeolite dose by 0.05 g whereas it is 1 g for zeolite A synthetized from fly ash [28] and 0.8 g for natural zeolites [2].

3.2.2. Effect of contact time

The influence of stirring time on the removal efficiency of metal ions was studied to determine the optimum contact time. The results are given on Fig. 4. As shown, sorption increases with increasing reaction time until the equilibrium was attained at 93%, 92% and 70% for Cu (II), Co (II) and Cr (III), respectively. We can also notice that the sorption took place rapidly in the first 60 min, which can be attributed to the availability of sites for the cations [29]. In fact, a very high adsorption driving force at the beginning helps in this rapid sorption. However, after the initial phase, slower adsorption may be assigned to the slower diffusion of cations into the interior pores of the zeolite [29], and the cations thereafter occupy the exchangeable positions in the crystal framework [30,31]. Optimal contact times were found to be 60 min for Cu and Co and 90 min for Cr.

Table 1
Textural properties of the FAU.

S_{BET} (m^2/g)	360
V_{total}[a] (cm^3/g)	0.33
V_{micro}[b] (cm^3/g)	0.0885
$S_{mesopores}$ (m^2/g)	126.4

FAU: faujasite type zeolite.
[a] Total pore volume calculated from nitrogen adsorption at $P/P_0 = 0.995$.
[b] Micropore volume calculated from nitrogen adsorption at $P/P_0 = 0.1$.

3.2.3. Effect of pH

The pH of the solution has a significant impact on the uptake of heavy metals since it may affect the ionization degree of the sorbate and the surface property of the sorbent [32]. Moreover, the selectivity of metal ion by zeolites is influenced by the character of the metal complex that predominates at a particular solution pH [33]. The contact of the zeolite surface with water leads to the ionization of surface hydroxyl groups (Si–OH and Al–OH). The degree of ionization is affected by pH, and the acid/base reaction taking place at the hydroxyl groups may results in surface charge development [34]. Zeolites are not only affected by pH but likewise are able of influencing solution pH especially in batch system and zeolites tend to have a higher internal pH. In fact, the zeolite surface may be influenced by the ambient pH, which is different from the external solution pH value and precipitation within the channels of zeolites and at the surface of zeolites may occur.

Fig. 5 illustrates the variation of Cu (II), Co (II) and Cr (III) removal on the synthesized zeolite at different pH values. The range of pH investigated was 2–9. Fig. 5 show that the

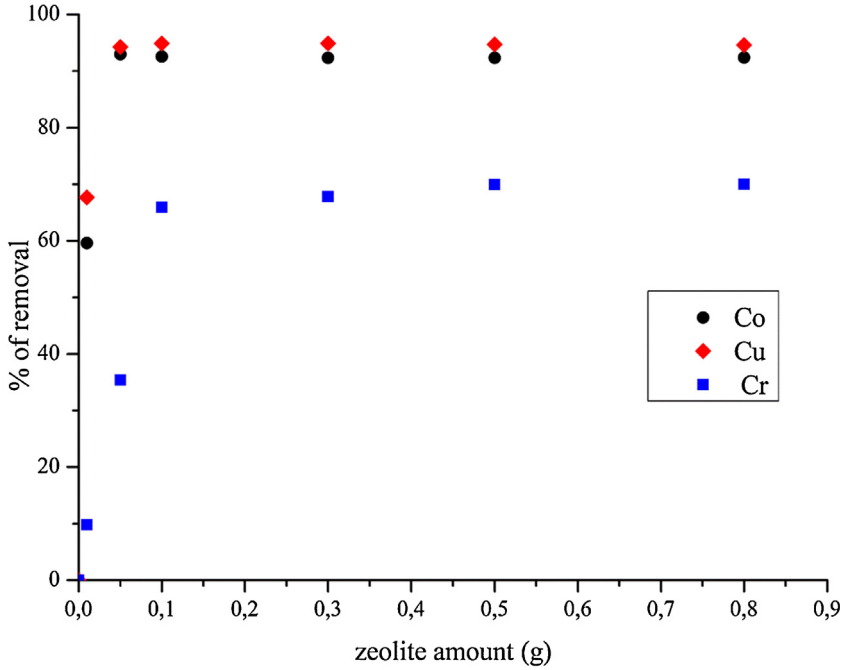

Fig. 3. (Color online.) Effect of faujasite type zeolite amount on the removal of heavy metal ions (C_0 = 50 mg/L, 150 rpm, V = 100 mL).

rate of adsorption of single metal ions increased with pH. In fact, the adsorption percentages increased clearly after pH 5 for all metals.

Copper ions adsorption remains almost constant up to 4, and then increased sharply to 94% adsorption around pH 6. At higher pH, the adsorption percentage was rather slow and decreased to 91% adsorption at pH 9. A similar behavior was observed for the sorption of chromium and cobalt ions where the adsorption percentage remains practically constant up to pH 5 and increase thereafter sharply. The maximum removal percentage for copper and chromium respectively were 90 and 71% at pH 6. These results are similar to results obtained by Abdel Salam et al. [35] for heavy metal ions sorption onto peanut husk

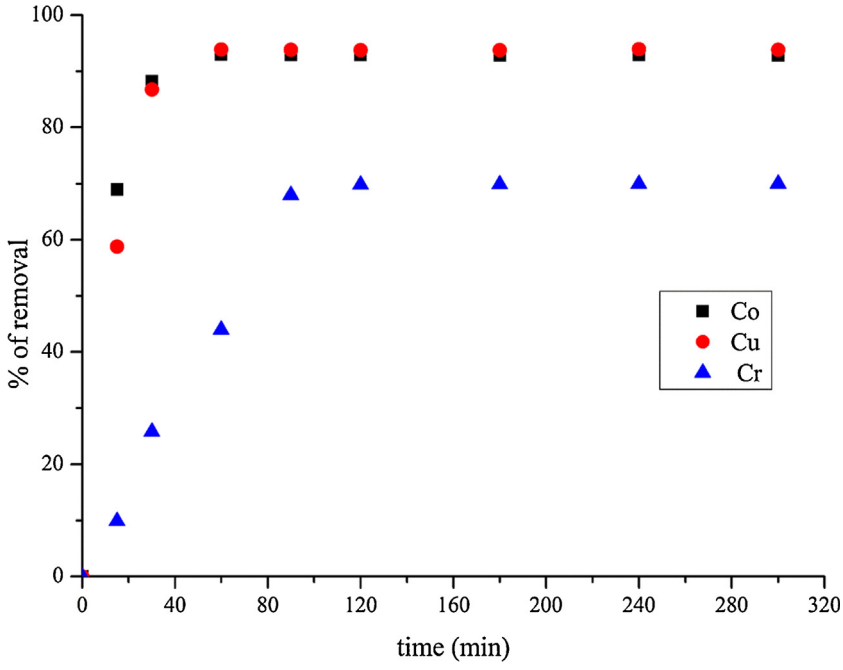

Fig. 4. (Color online.) Effect of contact time on the removal of heavy metal ions (C_0 = 50 mg/L, 150 rpm, V = 100 mL).

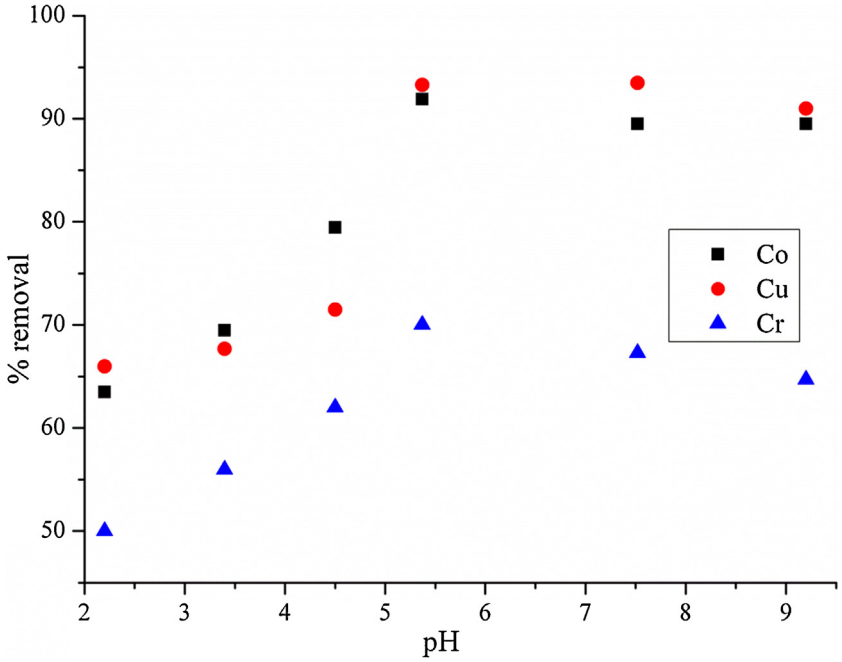

Fig. 5. (Color online.) Effect of pH on the removal of heavy metal ions (C_0 = 50 mg/L, m = 0.05 g, 150 rpm, V = 100 mL, t = 60 min).

charcoal and natural zeolite. Then, pH 6 was chosen as the optimum studying pH for all metals to avoid precipitation of metals.

In general, it is admitted that the adsorption of heavy metal ions raise with increasing the pH value [36]. Lower pH value cause an increase of H^+ ion concentration, which competes with metal ions for exchange sites in zeolitic adsorbents [37]. However, at pH higher than 6, majority of the heavy metal ions tend to precipitate which restrains the adsorption process. Thus, the adsorption of metals ions on zeolite is difficult to be quantified at the higher pH value than 6, and adsorption could be masked by precipitation [2].

3.3. Isotherm models

An adsorption isotherm equation is an expression of the relation between the proportion of solute adsorbed and the concentration of the solute in the fluid phase, since for solid–liquid system, the studies of adsorption isotherms are very important to realize information about adsorption capacity of adsorbents. Therefore, the correlation of equilibrium data using an equation is essential for practical adsorption operation [38]. In order to investigate the sorption isotherm, two equilibrium models were analyzed: Langmuir and Freundlich isotherm equations. These both isotherm models were first derived and used for gas adsorption by microporous adsorbents, and then extended to solute adsorption from aqueous solutions. The Langmuir model is obtained under the ideal supposition of a totally homogeneous adsorption surface, whereas the Freundlich isotherm is suitable for a highly heterogeneous surface [37].

3.3.1. Langmuir isotherm

The Langmuir model is the simplest and the most commonly-used model to represent the adsorption from a liquid phase by a solid phase [39]. This model assumes a monolayer adsorption.

It is represented as:

$$q_e = \frac{q_m K_L C_e}{1 + K_L C_e} \tag{2}$$

where C_e is the equilibrium aqueous metal ions concentration (mg/L), q_e the amount of metal ions adsorbed per gram of adsorbent at equilibrium (mg/g), q_m and K_L are the Langmuir constants related to the maximum adsorption capacity (mg/g) and energy of adsorption (L/mg), respectively.

The linear form of the Langmuir equation can be written as:

$$\frac{C_e}{q_e} = \frac{1}{K_L q_m} + \frac{C_e}{q_m} \tag{3}$$

The plots of $\frac{C_e}{q_e}$ versus C_e (not shown) are linear for all studied heavy metals, confirming the best fit with Langmuir model. These last plots yielded an important dimensionless parameter R_L, which is given by the equation:

$$R_L = \frac{1}{1 + K_L C_e} \tag{4}$$

For $0 < R_L < 1$, the adsorption is favorable.
For $R_L > 1$, the adsorption is unfavorable.
For $R_L = 1$, the equilibrium is linear.

3.3.2. Freundlich isotherm

The Freundlich isotherm is an empirical equation, which is used for the heterogeneous systems and is expressed as:

$$q_e = K_F C_e^{1/n} \quad (5)$$

where q_e is the amount of metal ions adsorbed at equilibrium (mg/g), C_e the equilibrium concentration in solution (mg/L). K_F and n are the Freundlich constants, characteristics of the system and indicators of adsorption capacity and reaction energy, respectively.

3.3.3. Adsorption isotherms

Fig. 6 shows the adsorption isotherms for Cu (II), Co (II) and Cr (III) onto the FAU at three different temperatures (25, 35 and 45 °C) fitted with the Langmuir and Freundlich models. The isotherm parameters determined by the Langmuir and Freundlich equations are shown in Table 2.

A detailed analysis of the correlation coefficients from Table 2 showed that Langmuir and Freundlich models adequately predicted the experimental data well for the adsorption of metal ions onto the synthesized zeolite. Nevertheless, Langmuir model presents slightly better correlation coefficients. Our results are similar to other reported papers, which studied the adsorption of heavy metals on activated carbon [40,41], on kaolinite and montmorillonite [42] and on agro-waste materials [43].

The fitting of sorption data to Langmuir sorption isotherm reveals that the coverage of metal ions examined on the surface of the zeolite may be defined as a monolayer adsorption with strong metal ion–sorbent interactions over the surfaces of FAU. The calculated values of R_L presented in Table 2 are all below 1, indicating that the adsorption of the Cu (II), Co (II) and Cr (III) onto the FAU is favorable.

In the other hand, we can notice that the values of saturation capacity q_m shown in Table 2 decreased when temperature increased for all the cases due to reduce in adsorption capacities at higher temperatures. That is confirming the exothermic nature of adsorption of the studied heavy metals on the FAU. Moreover and according to the q_m values of the Langmuir model, the maximum monolayer adsorption capacity of FAU follows the order: Cu (II) > Co (II) > Cr (III) by 126, 125 and 98 mg/g, respectively. These adsorption capacities are interesting because the same experiments applied on the commercial FAU from "Zeolyst International CBV100" showed lower values: Cu (II) > Co (II) > Cr (III) by 120, 118 and 91 mg/g, respectively.

Moreover, several selectivity series have been reported in the literature for natural and synthesized zeolite [44–46]. Our results are similar to most of previous reports. The observed differences could be attributed to the specificity of the adsorbents and to the difference in the experimental techniques used [47]. In fact, factors such as crystal structure of zeolite, free energy of hydration and hydrated radii of the metal ions may are the key factors of observed selectivity for each studied zeolite [48]. In the present study, the adsorption capacities follow the size of hydrated radii of ions, 4·19 Å, 4.23 Å and 4.61 Å for Cu (II), Co (II) and Cr (III), respectively.

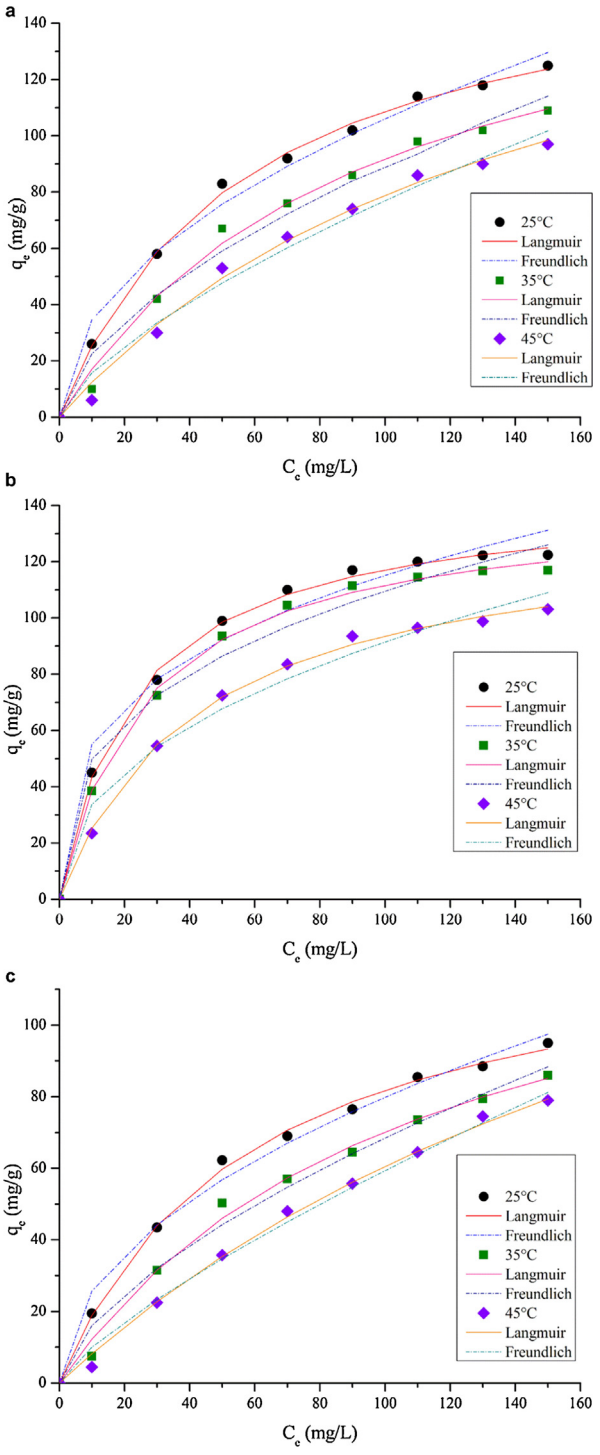

Fig. 6. (Color online.) Experimental data fitting to Langmuir and Freundlich isotherms for (a) copper (Cu) (II), (b) cobalt (Co) (II) and (c) chromium (Cr) (III) ions.

3.3.4. Isosteric heat of adsorption

In the thermodynamics of adsorption, important information is given by adsorption isosteres, which are temperature dependent of the concentration of the

Table 2
Langmuir and Freundlich parameters for Cu (II), Co (II) and Cr (III) ions.

Element	Temperature (°C)	Langmuir					Freundlich		
		q_{exp}	q_m	K_L	R_L	R^2	K_F	$1/n$	R^2
Cu (II)	25	125	126	0.017	0.816	0.999	11.27	0.486	0.995
	35	116	117	0.012	0.855	0.997	5.65	0.599	0.991
	45	103	110	0.006	0.888	0.997	3.21	0.689	0.992
Co (II)	25	122	125	0.047	0.658	0.999	26.34	0.322	0.992
	35	109	115	0.033	0.681	0.999	22.59	0.342	0.991
	45	97	107	0.027	0.778	0.999	12.41	0.433	0.999
Cr (III)	25	95	98	0.017	0.853	0.999	8.30	0.491	0.996
	35	86	90	0.009	0.895	0.997	3.77	0.629	0.993
	45	79	83	0.004	0.950	0.998	1.24	0.773	0.997

Cu: copper; Cr: chromium; Co: cobalt.

equilibrium phase for a constant amount of metal ions adsorbed.

The experimental results obtained were used for calculation of differential heats of adsorption by means of the Clausius–Clapeyron equation.

$$\frac{d(\ln C_e)}{dT} = -\frac{\Delta H}{RT^2} \quad (6)$$

where C_e is the equilibrium concentration at constant amount of adsorbed metal ions (mol/L) that can be obtained from the sorption data at different temperatures. ΔH (KJ/mol) can be calculated from the slope of a plot of ln C_e versus $1/T$ [49].

Plots of ln C_e versus $1/T$ for different amounts of metals ions adsorption were found to be linear and the results for the cobalt ions are given on Fig. 7. The values of the isosteric heat of adsorption (data obtained but not shown) were measured from the slope of the linearized form of Clausius–Clapeyron equation. According to this, it was found that ΔH values calculated in the temperature range of 25–45 °C indicate that physisorption is involved in Cu (II), Co (II) and Cr (III) sorption [49] and the linear character of the isosteres constructed means that the physical adsorption process does not significantly change with an increase in temperature.

3.4. Kinetic study

Various mechanisms, such as mass transfer, particle diffusion, and chemical reactions control the process of adsorption. Several models have been developed to examine experimental data and explain the adsorption process. The kinetic data of the adsorption of Cu, Co and Cr was evaluated using pseudo-first-order and pseudo-second-order models. The pseudo-first-order kinetics can be generally described in the following equation:

$$\ln(q_e - q_t) = \ln q_e - K_1 t \quad (7)$$

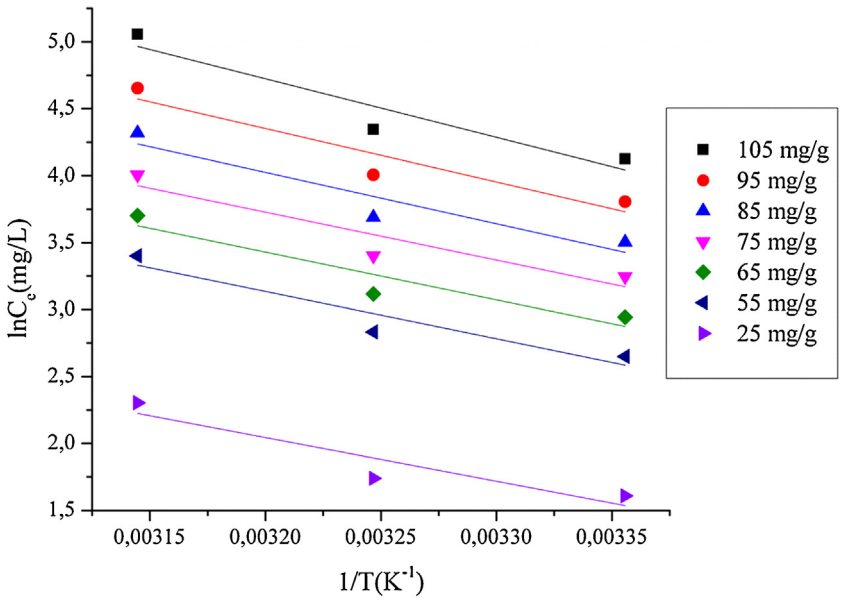

Fig. 7. (Color online.) Isosteres for different adsorbed amounts of cobalt (Co) (II) ions.

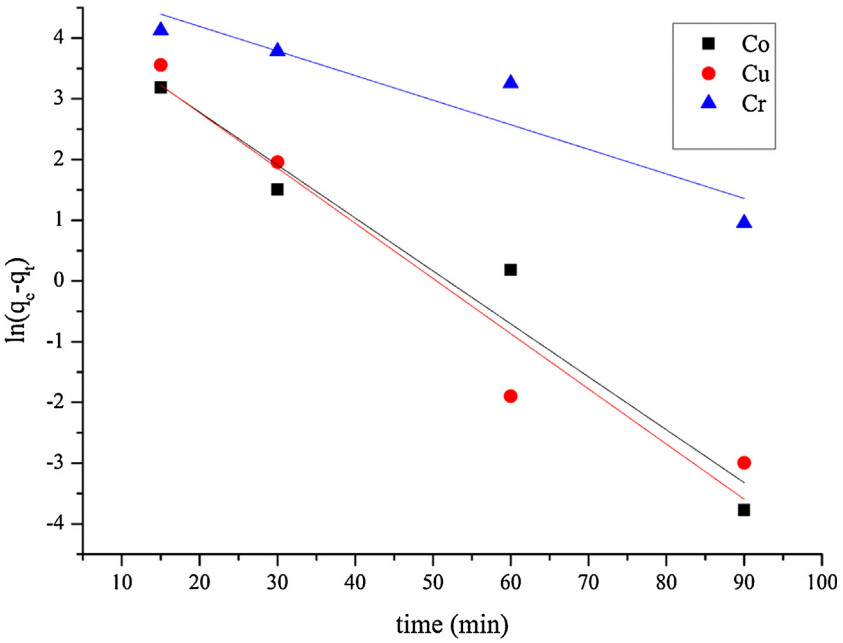

Fig. 8. (Color online.) Pseudo-first-order kinetic plot for the adsorption of copper (Cu) (II) ions, cobalt (Co) (II) and chromium (Cr) (III) ions onto zeolite faujasite type zeolite.

where q_e and q_t are the amounts (mg/g) of adsorbed metal ions FAU at equilibrium and at time t, respectively. K_1 is the first-order rate constant (1/min).

The value of K_1, q_e and correlation coefficient R^2 could be calculated from the slope and intercept of the linear plot of ln (q_e–q_t) versus t, respectively (Fig. 8). The results are summarized in Table 3.

The pseudo-second-order model is expressed as:

$$\frac{t}{q_t} = \frac{1}{K_2 q_e^2} + \frac{1}{q_e} t \qquad (8)$$

where K_2 is the constant of pseudo-second-order rate (g/mg·min), q_e is the amount adsorbed at equilibrium, and q_t is the amount adsorbed at time t. The equilibrium adsorption amount (q_e), the pseudo-second-order rate parameters (K_2) and the correlation coefficient R^2 can be obtained from the slope and intercept of plot of t/q_t versus t (Fig. 9). The corresponding values are presented in Table 3.

The K_2 value calculated from the slope and intercept are 2.761×10^{-3}; $5 \times 13 \times 10^{-3}$ and 2.78×10^{-4} for the Cu, Co and Cr ions, respectively. The low values of rate constant (K_2) suggested that the adsorption rate decreased with the increase in time and the adsorption rate was proportional to the number of unoccupied sites [50,51]. The regression coefficients for the pseudo-second-order were relatively high compared to the pseudo-first-order, suggesting that the experimental kinetic data fits better to the pseudo-second-order model. Furthermore, the estimated q_e values (Table 3), using the pseudo-second-order model, are in good agreement with the experimental values q_{exp}. Thus, the empirical second-order model was more appropriate to represent the experimental kinetic data in the adsorption system. It seems that the rate-limiting step is chemical adsorption and the adsorption behavior may implicate valency forces through sharing electrons between transition metal cations and adsorbent [39,52].

3.5. Comparison with other studies

Table 4 shows the comparison of results obtained in this study with other reported in previous studies. It can be

Table 3
Kinetic parameters of heavy metal adsorption by pseudo-first-order, pseudo-second-order.

Metal	q_{exp} (mg/g)	Pseudo-first-order			Pseudo-second-order		
		q_e (mg/g)	K_1 (1/min)	R^2	q_e (mg/g)	K_2 (g/mg·min)	R^2
Cu (II)	93	98	0.0159	0.946	90	0.0027631	0.999
Co (II)	92	92	0.015	0.956	90	0.0051337	0.999
Cr (III)	69	82	0.071	0.886	74	0.00027787	0.962

Cu: copper; Cr: chromium; Co: cobalt.

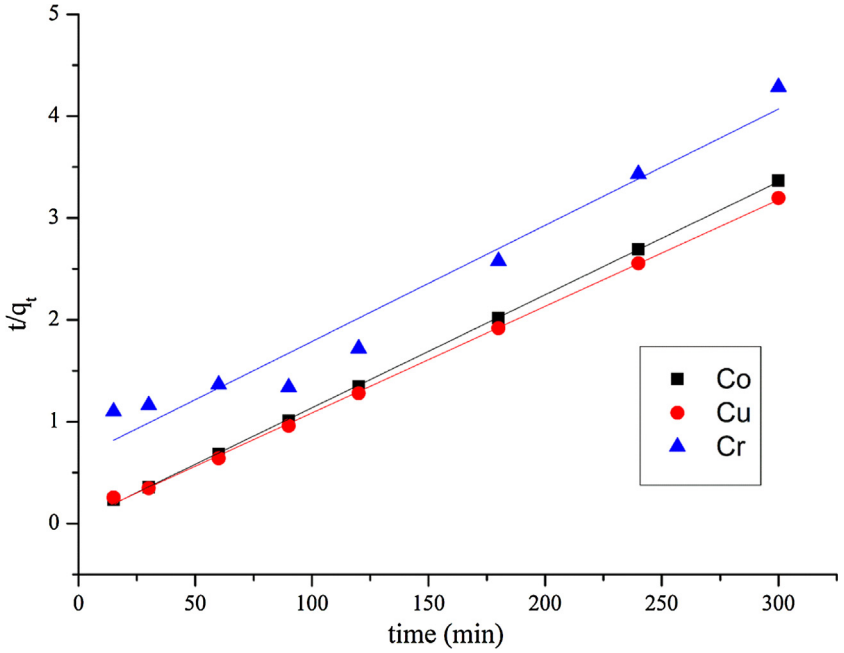

Fig. 9. (Color online.) Pseudo-second-order kinetic plot for the adsorption of copper (Cu) (II) ions, cobalt (Co) (II) and chromium (Cr) (III) ions onto zeolite faujasite type zeolite.

seen that that the FAU prepared from IC had exceptionally a high capacity for heavy metals removal in comparison with many other adsorbents such as zeolite A [28], natural zeolite [3], phosphonic resin [54], hull ash [57]. The high adsorption capacities suggest that FAU prepared from IC is a powerful adsorbent for the removal of heavy metals ions from wastewater. In fact, differences of metal uptake are due to the properties of each sorbent material such as structure, functional groups and surface proprieties. The improved adsorption capacities toward Cu (II), Co (II) and Cr (III) ions of our material could be attributed to its high specific surface area and its important hierarchical porosity.

Table 4
Comparison of Cu (II), Co (II) and Cr (III) sorption capacity with other adsorbents.

Metal	Adsorbent/sorbent	C_0 (mg/L)	q_{max} (mg·g^{-1})	Literature
Cu (II)	Faujasite zeolite	150	125	This work
	Zeolite A	200	82	[28]
	Natural zeolite tuff	150	20	[3]
	Zeolite Na-A	150	129	[53]
	Phosphonic resin	250	85	[54]
Co (II)	Faujasite zeolite	150	122	This work
	Hydroxyapatite	100	20	[55]
	Boron waste	300	63	[56]
Cr (III)	Faujasite type zeolite	150	73	This work
	Rice hull ash	100	4	[57]

Cu: copper; Cr: chromium; Co: cobalt.

4. Conclusion

Natural illitic Tunisian clay was successfully valorized for the production of zeolitic material. The specific surface area of the as-synthesized zeolite was of 360 m^2/g and the total pore size 0.33 cm^3/g and the porosity is hierarchical. The obtained results showed that FAU material exhibits effective adsorption for Cu (II), Co (II) and Cr (III) ions in aqueous solution, with adsorption capacities in the order Cu (II) > Co (II) > Cr (III) in a single component system. The equilibrium data have been fitted using Freundlich and Langmuir equation model. The Langmuir isotherm was demonstrated to provide the best correlation. The suitability of pseudo-first- and second-order kinetic models for the adsorption of heavy metals onto optimum composition was also studied. The pseudo-second-order kinetic model agrees very well with the adsorption behavior of the three heavy metals. This new material could be successfully used to treat wastewater polluted with heavy metal.

Acknowledgments

The authors are grateful to PHC Maghreb No. 27959PD for financial support and to the scientific partnership between the "École nationale d'ingénieurs de Sfax" (Tunisia) and the "Université du Littoral Côte d'Opale Dunkerque" (France) for financial support to Olfa Ouled Ltaief's PhD thesis.

References

[1] M.A. Shavandi, Z. Haddadian, M.H.S. Ismail, N. Abdullah, Z.Z. Abidin, J. Taiwan Inst. Chem. Eng. 43 (2012) 750–759.

[2] S. Kocaoba, Y. Orhan, T. Akyüz, Desalination 214 (2007) 1–10.
[3] S. Wang, T. Terdkiatburana, M.O. Tad'e, Sep. Purif. Technol. 62 (2008) 64–70.
[4] S. Rengaraj, S.H. Moon, Water Res. 36 (2002) 1783–1793.
[5] M. Suwalsky, R. Castro, F. Villena, C.P. Sotomayor, J. Inorg. Biochem. 102 (2008) 842–849.
[6] J. Mizera, G. Mizerova, V. Machovic, L. Borecka, Water Res. 41 (2007) 620–626.
[7] V.K. Gupta, C.K. Jain, I. Ali, M. Sharma, V.K. Saini, Water Res. 37 (2003) 4038–4044.
[8] A. Ahmadpour, M. Tahmasbi, T. RohaniBastami, J. Amel Besharati, J. Hazard. Mater. 166 (2009) 925–930.
[9] J. Oliva, J.D. Pablo, J.-L. Cortina, J. Cama, C. Ayora, J. Hazard. Mater. 194 (2011) 312–323.
[10] Y.A. Zheng, D.J. Huang, A.Q. Wang, Chim. Acta 687 (2011) 193–200.
[11] P. Sharma, M. Sharma, R. Tomar, J. Taiwan Inst. Chem. Eng. 44 (2013) 480–488.
[12] D. Novembre, B. DiSabatino, D. Gimeno, M. Garcia-Vallès, S. Manent, Microporous Mesoporous Mater. 75 (2004) 1–11.
[13] M. Meznia, A. Hamzaoui, N. Hamdi, E. Srasra, Appl. Clay Sci. 52 (2011) 209–218.
[14] A. Duana, G. Wanb, Y. Zhang, Z. Zhao, G. Jiang, J. Liu, Catal. Today 175 (2011) 485–493.
[15] N. Shigemoto, H. Hayashi, K. Miyaura, J. Mater. Sci. 28 (1993) 4781–4786.
[16] H. Liu, S. Peng, L. Shu, T. Chen, T. Bao, R.L. Frost, Chemosphere 91 (2013) 1539–1546.
[17] T.S. Jamil, H.S. Ibrahim, I.H. Abd El-Maksoud, S.T. El-Wakeel, Desalination 258 (2010) 34–40.
[18] C.R. Meloa, H.G. Riella, N.C. Kuhnen, E. Angioletto, A.R. Meloc, A.M. Bernardin, M.R. da Rocha, L. da Silva, Mater. Sci. Eng., B ADV177 (2012) 345–349.
[19] M. Eloussaief, N. Kallel, A. Yaacoubi, M. Benzina, Chem. Eng. J. 168 (2011) 1024–1031.
[20] I. Jarraya, S. Fourmentin, M. Benzina, S. Bouaziz, Chem. Geol. 275 (2010) 1–8.
[21] N. Dammak, O. Ouledltaief, N. Fakhfakha, M. Benzina, Surf. Interface Anal. 46 (2014) 457–464.
[22] Y. Huang, K. Wang, D. Dong, D. Li, M.R. Hill, A.J. Hill, H. Wang, Microporous Mesoporous Mater. 127 (2010) 167–175.
[23] E. Erdem, N. Karapinar, R. Donat, J. Colloid Interface Sci 280 (2004) 309–314.
[24] A.M. El-Kamash, A.A. Zaki, M. Abed El Geleel, J. Hazard. Mater. 127 (2005) 211–220.
[25] S. Wang, E. Ariyanto, J. Colloid Interface Sci. 314 (2007) 25–31.
[26] R.G. Casqueira, M.L. Torem, H.M. Kohler, Miner. Eng. 19 (2006) 1388–1392.
[27] S. Mohan, R. Gandhimathi, J. Hazard. Mater. 169 (2009) 351–359.
[28] C. Wang, J. Li, X. Sun, L. Wang, X. Sun, J. Environ. Sci. 21 (2009) 127–136.
[29] T. Motsi, N.A. Rowson, M.J.H. Simmons, Int. J. Miner. Process. 101 (2011) 42–49.
[30] T. Calvete, E.C. Lima, N.F. Cardoso, S.L.P. Dias, F.A. Pavan, Chem. Eng. J. 155 (2009) 627–636.
[31] E.-S. Gamal Owes, Desalination 272 (2011) 225–232.
[32] H. Cho, D. Oh, K. Kim, J. Hazard. Mater. 127 (2005) 187–195.
[33] S.K. Ouki, M. Kavannagh, Waste Manage. Res. 15 (1997) 383–394.
[34] C. Covarrubias, R. Arriagada, J. Yanez, R. Garcia, M. Angelica, S.D. Barros, P. Arroyo, E.F. Sousa-Aguiar, J. Chem. Technol. Biotechnol. 80 (2005) 899–908.
[35] O.E. Abdel Salam, N.A. Reiad, M.M. ElShafei, J. Adv. Res. 2 (2011) 297–303.
[36] C.P. Huang, F.B. Ostovic, J. Environ. Eng. 104 (1978) 863–878.
[37] K.S. Hui, C.Y.H. Chao, S.C. Kot, J. Hazard. Mater. 127 (2005) 89–101.
[38] M.A. Hashem, Int. J. Phys. Sci. 2 (2007) 178–184.
[39] V.M. Boddu, K. Abburi, J.L. Talbott, E.D. Smith, Environ. Sci. Technol. 37 (2003) 4449–4456.
[40] T. Terdkiatburana, S. Wang, M.O. Tadé, Chem. Eng. J. 139 (2008) 437–444.
[41] A. Üçer, A. Uyanik, S.F. Aygün, Sep. Purif. Technol. 47 (2006) 113–118.
[42] S.S. Guptaa, K.G. Bhattacharyya, J. Environ. Manage. 87 (2008) 46–58.
[43] R.B. Garcia-Reyes, J.R. Rangel-Mendez, Bioresour. Technol. 101 (2010) 8099–8108.
[44] M.J. Zamzow, L.E. Schultze, in: D.W. Ming, F.A. Muphton (Eds.), Natural Zeolites'93: Occurrence, Properties, Use, Brockport, New York, 1995, pp. 405–413.
[45] G. Blanchard, M. Maunaye, G. Martin, Water Res. 18 (1984) 1501–1507.
[46] E. Alvarez-Ayuso, A. Garcia-Sanchez, X. Querol, Water Res. 37 (2003) 4855–4862.
[47] M. Majdan, S. Pikus, M. Kowalska-Ternes, A. Gladysz-Plaska, P. Staszczuk, L. Fuks, H. Skrzypek, J. Colloid Interface Sci. 262 (2003) 321–330.
[48] A. Esposito, F. Pagnanelli, A. Lodi, C. Solisio, F. Veglio, Hydrometallurgy 60 (2) (2001) 129–141.
[49] T.S. Anirudhan, P.G. Radhakrishnan, J. Chem. Thermodyn. 40 (2008) 702–709.
[50] P. Xu, G.M. Zeng, D.L. Huang, C. Lai, M.H. Zhao, Z. Wei, N.J. Li, C. Huang, G.X. Xie, Chem. Eng. J. 203 (2012) 423–431.
[51] V.K. Gupta, A. Rastogi, A. Nayak, J. Colloid Interface Sci. 342 (2010) 533–539.
[52] G.W. Yang, H.Y. Han, C.Y. Du, Z.H. Luo, Y.J. Wang, Polymer 51 (2010) 6193–6202.
[53] B. Weiwei, L. Lu, Z. Haifeng, G. ShucDi, X. Xuechun, J. Guijuan, G. Guimeiand, Z. Keyan, Chin. J. Chem. Eng. 21 (2013) 974–982.
[54] M.D. Rabiul Awual, T. Yaita, Y. Okamoto, Sens. Actuators, B Chem. 203 (2014) 71–80.
[55] I. Smičiklas, S. Dimović, I. Plećaš, M. Mitrić, Water Res. 40 (2006) 2267–2274.
[56] A. Olgun, N. Atar, Chem. Eng. J. 167 (2011) 140–147.
[57] L. Hua Wang, C. Lin, J. Taiwan Inst. 39 (2008) 367–373.